Biochimica et Biophysica Acta 1818 (2012) 2572–2578

Contents lists available at SciVerse ScienceDirect

Biochimica et Biophysica Acta

journal homepage: www.elsevier.com/locate/bbamem

Lipid interactions of the malaria antigen merozoite surface protein 2

Christopher A. MacRaild [a,1], Marie Ø. Pedersen [a,1], Robin F. Anders [b], Raymond S. Norton [a,*]

[a] Medicinal Chemistry, Monash Institute of Pharmaceutical Sciences, Monash University, 381 Royal Parade, Parkville 3052, Australia
[b] Department of Biochemistry, La Trobe University, Victoria 3086, Australia

ARTICLE INFO

Article history:
Received 23 April 2012
Received in revised form 20 June 2012
Accepted 21 June 2012
Available online 27 June 2012

Keywords:
Malaria
Plasmodium falciparum
Merozoite surface protein 2
Structure
NMR

ABSTRACT

With more than half the world's population living at risk of malaria infection, there is a strong demand for the development of an effective malaria vaccine. One promising vaccine candidate is merozoite surface protein 2 (MSP2), which is among the most abundant antigens of the blood stage of the *Plasmodium falciparum* parasite. In solution, MSP2 is intrinsically unstructured, but little is known about the conformation of native MSP2, which is GPI-anchored to the merozoite surface, or of the implications of that conformation for the immune response induced by MSP2. Initial NMR studies have shown that MSP2 interacts with lipid micelles through a highly conserved N-terminal domain. We have further developed these findings by investigating how different lipid environments affect the protein structure. All of the tested lipid preparations perturbed only the N-terminal part of MSP2. In DPC micelles this region adopts an α-helical structure which we have characterized in detail. Our findings suggest a possible mechanism by which lipid interactions might modulate immune recognition of the conserved N-terminus of MSP2, potentially explaining the apparent immunodominance of the central variable region of this important malaria antigen.

1. Introduction

Antigens on the surface of the *Plasmodium falciparum* merozoite represent attractive candidates for inclusion in a malaria vaccine [1]. Merozoite surface protein 2 (MSP2) is a ~28 kDa protein anchored to the merozoite membrane by a C-terminal glycosylphosphatidylinositol (GPI) moiety [2] and is one of the most abundant proteins on the surface of the merozoite [3]. Because of its localisation at the merozoite surface, MSP2 is directly accessible to immune recognition by plasma antibodies. People naturally-exposed to malaria acquire high levels of anti-MSP2 antibodies and these responses have been associated with protection from symptomatic disease [4–9]. For these reasons, vaccines incorporating MSP2 are under active development [1,10,11]. Recent clinical trials of MSP2-based vaccines have established their safety and partial efficacy, but have highlighted the need to induce a response that better matches the specificity of the naturally acquired response [11,12].

MSP2 exists as one of two major allelic types, FC27 and 3D7, which are distinguished by the sequences of a highly polymorphic central region that consists of non-repeat sequences surrounding tandem repeat sequences [13,14]. FC27 forms of MSP2 contain 32-residue and 12-residue repeats, whereas 3D7 forms of the antigen contain much shorter repeats. The diversity of the central regions is likely to have evolved under immune pressure from the human host [14]. All MSP2 alleles have conserved 25-residue N-terminal and ~50-residue C-terminal amino acid sequences that flank the central variable region (Fig. 1, Supplementary Figure S1). An MSP2 construct has been expressed in *E. coli* where the central variable region was deleted, leaving the N- and C-terminal domains joined directly. This recombinant construct is immunogenic, but the antibodies raised have a different specificity from those in naturally-infected hosts, and the protein was poorly recognised by sera from malaria-exposed humans that are reactive against native MSP2 [15]. These results suggest that the N- and C- terminal regions of MSP2 are not exposed to the human immune system in the course of a natural malaria infection. Recently, we have characterised a panel of monoclonal antibodies raised against recombinant MSP2. Of this panel, most of those that recognise the conserved regions of recombinant MSP2 either fail to recognise, or react poorly with, MSP2 on the parasite surface, whereas those that recognise the central variable region of MSP2 react well with the parasite surface [16].

Recombinant MSP2 is intrinsically unstructured, with a high propensity for fibril formation [17,18]. Like many malaria surface antigens, MSP2 is GPI anchored to the merozoite surface. However, the structural characteristics of MSP2 on the merozoite surface remain unknown. GPI-mediated lipid interactions alter the antigenic properties of proteins of other parasitic organisms [19], but these issues have not been addressed in the case of MSP2 or other malaria antigens. Recently, we have shown that the conserved N-terminal region of MSP2 interacts with dodecyl phosphocholine (DPC) micelles, in the

Abbreviations: MSP2, merozoite surface protein 2; DPC, dodecyl phosphocholine; LPPG, lyso-palmatoyl phosphatidylglycerol; DLPC, dilauryl phosphatidylcholine; SUVs, small unilamellar vesicles

* Corresponding author. Tel.: +61 3 9903 9167; fax: +61 3 9903 9582.
E-mail address: ray.norton@monash.edu (R.S. Norton).

[1] Contributed equally.

0005-2736/$ – see front matter © 2012 Elsevier B.V. All rights reserved.
doi:10.1016/j.bbamem.2012.06.015

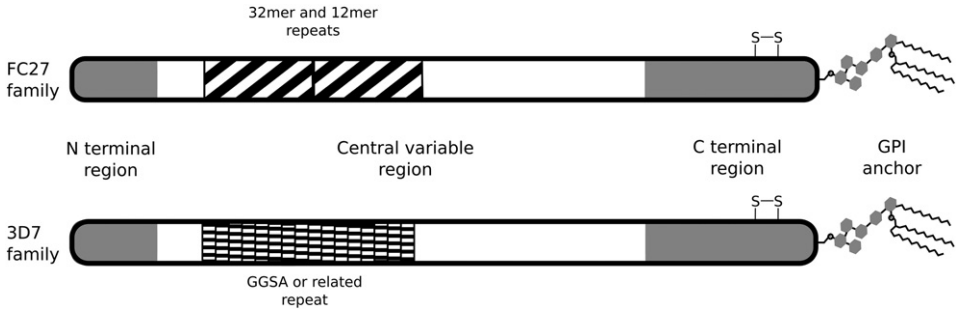

Fig. 1. Schematic of the two families of MSP2, FC27 and 3D7.

absence of the GPI anchor [18]. This raises the possibility that lipid interactions may play a role in determining the apparent immunodominance of the central variable region of MSP2. Here we undertake a detailed structural characterisation of the interaction of MSP2 with lipid surfaces, in order to understand the implications for the interactions of MSP2 with the host immune system and with a view to designing more effective MSP2-based malaria vaccines.

2. Experimental procedures

2.1. Materials

All studies described here were carried out with the recombinant FC27 allelic form of MSP2 expressed in *E. coli*. Untagged full-length FC27 MSP2 was expressed and purified using a strategy specific for recombinantly expressed unstructured proteins, as described previously [18]. Truncated FC27 MSP2 ($MSP2_{1\text{-}25}$) was either expressed and purified according to the protocol by Low et al. [20] or purchased as a synthetic peptide from GL Biochem (Shanghai, China). ^{15}N-labelled full-length or truncated MSP2 was prepared by growing expression cultures in M9 minimal medium, with 1 g/L ^{15}N ammonium chloride as the sole nitrogen source.

2.2. Sample preparation

All MSP2 samples used in titration experiments were freshly prepared by dissolution of freeze-dried MSP2 in the appropriate buffer and briefly heated to 95 °C to dissolve any aggregates present. Working stocks of $^{2}H_{38}$-DPC (Cambridge Isotope Laboratories) and LPPG (Avanti Polar Lipids) were freshly prepared in the appropriate buffer. Lipid SUVs were prepared by suspending dry DLPC (Avanti Polar Lipids) in buffer and subjecting the mixture to probe sonication and vortex mixing until a stable transparent solution was achieved. $MSP2_{1-25}$ samples for structure determination were prepared by dissolution of freeze-dried peptide directly in the buffered DPC solution (50 mM DPC, 20 mM sodium acetate, pH 4.5).

2.3. NMR spectroscopy

Samples for NMR spectroscopy contained 5% $^{2}H_2O$ and 0.01% dioxane, the latter as an internal reference for chemical shift and diffusion coefficient measurements. NMR spectra were acquired on Bruker Avance 500 and 600 MHz spectrometers equipped with cryoprobes, and a Bruker DRX-600 spectrometer with a room-temperature probe. ^{1}H chemical shifts were referenced with dioxane set as 3.751 ppm, and ^{15}N and ^{13}C chemical shifts were referenced indirectly from ^{1}H using the ratios $\gamma_N/\gamma_H = 0.101329118$ and $\gamma_C/\gamma_H = 0.251449453$ [21]. Two-dimensional ^{1}H-^{15}N HSQC spectra were typically acquired with 2048 (^{1}H) and 256 (^{15}N) points and spectral widths of 9 ppm (^{1}H) and 24 ppm (^{15}N). Diffusion measurements were performed using a pulsed field gradient longitudinal eddy-current delay pulse sequence, as implemented by Yao et al. [22]; a series of 12 spectra was acquired with the strength of the diffusion gradient varying from 3.44 G cm^{-1} to 36.22 G cm^{-1}. NMR Spectra were processed using Bruker Topspin or NMRpipe [23], and assignment of $MSP2_{1-25}$ was done in SPARKY [24].

2.4. Structure calculation

A structural ensemble of $MSP2_{1\text{-}25}$ was calculated based on NOE restraints derived from the 2D NOESY spectrum. Calibration of NOE distance restraints and initial structure calculations were carried out using CYANA (version 1.0.6). φ-angles were restricted to negative values ($-90° \pm 90°$) [25], and, for residues shown by chemical shift and NOE patterns to be in the α-helical region of $MSP2_{1-25}$, the φ and ψ angles were restricted further to $-64° \pm 30$ and $-40° \pm 30°$, respectively. Final structure calculations were performed in NIH-XPLOR [26], with 100 conformers calculated with high temperature simulated annealing in torsion angle space followed by extensive Cartesian annealing and refinement. The final ensemble of 20 structures was selected on the basis of overall XPLOR energy, with the exclusion of structures with an NOE energy term exceeding 10 kcal/mol; this later filter being required to exclude a small number of low-energy structures with anomalously high NOE energy due to an obvious distortion around residue 15 in violation of several short-range NOEs (Table 1). The structure was validated using PROCHECK [27], with RMSD values and angular order parameters calculated using MOLMOL [28], and other structural analysis using PyMOL [29].

3. Results

3.1. MSP2–micelle interactions

We have previously shown that under acidic conditions, recombinant MSP2 lacking the C-terminal GPI anchor, interacts with zwitterionic DPC micelles, despite its marked hydrophilic character [18]. To further characterise this interaction, we performed DPC titrations under acidic (pH 3.5 and 4.5) and neutral (pH 7.3) conditions, using ^{1}H– ^{15}N HSQC spectra of MSP2 to monitor the interaction. Under all of the conditions tested we saw no change to MSP2 spectra in the presence of DPC below its critical micelle concentration (CMC) of ~1 mM, indicating that MSP2 does not interact with isolated molecules of DPC (data not shown). In contrast, we observed significant changes at micellar concentrations as MSP2 interacted with the DPC micelle. This interaction caused substantial line-broadening and chemical shift perturbation involving the entire conserved N terminal region, and a few residues at the extreme C-terminus. No changes in either chemical shift or line-shape were observed for residues in the central variable region, or in most of the C-terminal region, indicating that these parts of MSP2 do not interact with the DPC micelle and are not significantly perturbed by the interaction of the N-terminus. The lack of line-broadening in these regions is consistent with the highly flexible nature of MSP2 [18], and indicates that these residues are conformationally decoupled from the DPC micelle, even when the N-terminal part of the molecule is bound.

At low pH and low DPC concentrations the spectral changes in the N-terminal region were dominated by chemical shift changes, indicative of an interaction that is in fast exchange on the chemical shift timescale. As the DPC concentration was increased, line-broadening became more significant, to the extent that at 50 mM DPC, where the interaction nears saturation, approximately 50% of affected resonances were broadened beyond detection (Fig. 2A). The chemical shift perturbations due to DPC showed a uniform dependence on DPC concentration over all perturbed resonances (Fig. 2B), and in both ^{1}H and ^{15}N chemical shift, indicative of a simple two-state exchange between free MSP2 and a single DPC-bound state.

Near neutral pH, the DPC titration affected an identical set of MSP2 residues at the N-terminus. In contrast to the low-pH case, these data are characterised by very few observable chemical shift perturbations, but rather by line-broadening throughout the conserved N-terminal region (Figs. 2C and 3B). This line broadening may be attributed either to exchange processes occurring on an intermediate timescale or to the intrinsic relaxation properties of the relatively large DPC-MSP2 complex. We favour the former explanation because, as argued above, the DPC micelle is conformationally decoupled from the bulk of the bound MSP2 molecule. Therefore we expect the rotational diffusion, and thus the NMR relaxation, of the DPC micelle to be largely unperturbed by the bulk of the MSP2 molecule. Intermediate timescale exchange at neutral pH may reflect a slightly higher affinity of MSP2 for the micelle under these conditions.

3.2. Lipid induced MSP2 oligomer-formation

For all of the conditions we considered, line-broadening impeded our ability to characterise structural details of the interaction of full-length MSP2 with DPC micelles. For this reason, we chose to investigate the interaction of MSP2 with the acidic lysopalmitoylphosphatidyl glycerol (LPPG), which has yielded high-quality NMR spectra for other challenging protein-lipid complexes [30,31].

Despite the markedly different head-group chemistry, the N-terminal region of MSP2 interacts with LPPG micelles at neutral pH in a manner similar in many respects to its interactions with DPC. Specifically, we observe marked line-broadening of most resonances in the N-terminal region of MSP2, with only a few small chemical shift perturbations (Fig. 3). Strikingly, and in contrast to the case with DPC, the LPPG-induced changes to the MSP2 spectra were observed at low protein:LPPG ratios. Widespread line-broadening was observed for the MSP2 N-terminus even at sub-stoichiometric concentrations of LPPG, and all spectral changes were observed to saturate at MSP2:LPPG ratios around 1:5 (data not shown). The CMC of LPPG is approximately 50 μM, 3–5 fold lower than the MSP2 concentrations used in these studies, and the LPPG micelle comprises ~125 molecules [32]. Thus a micellar complex under these conditions would contain ~25 MSP2 molecules. A more plausible interpretation of these results is that MSP2 disrupts LPPG micelles and interacts with sub-micellar lipid complexes. Similar behaviour was observed for the MSP2-LPPG interaction at pH 4.5 (data not shown).

In an attempt to further characterise these complexes, we measured diffusion coefficients for MSP2 in the presence of increasing LPPG concentrations. The translational diffusion coefficient for MSP2 alone under these conditions was 3.2×10^{-11} cm^2/s, and addition of LPPG in 2.5-fold molecular excess reduced the diffusion coefficient to 2.4×10^{-11} cm^2/s, while further addition of LPPG caused only a small further reduction, to 2.3×10^{-11} cm^2/s. Thus the addition of LPPG caused an approximately 40% increase in the effective hydrodynamic radius of MSP2. In contrast, binding to DPC micelles caused a less than 20% increase [18]. These results imply that MSP2 forms oligomeric complexes stabilised by non-micellar LPPG. Such an interaction is in some respects similar to the complexes formed by α-synuclein in the presence of low lipid concentrations [33]. Attempts to measure the diffusion of LPPG in these complexes were unsuccessful, due to relaxation losses during the diffusion encoding delay. This is not the case for LPPG micelles in the absence of MSP2, which under the same conditions (1 mM in LPPG monomers) showed a significantly higher diffusion coefficient of 4.3×10^{-11} cm^2/s, further emphasising that the properties of the LPPG-MSP2 complex are markedly distinct from those of LPPG micelles.

3.3. MSP2–lipid bilayer interactions

To address the implications of lipid interactions for MSP2 on the merozoite surface, we probed the interaction of MSP2 with lipid bilayers in the form of DLPC SUVs. Given the large size of these vesicles, we expected resonances corresponding to lipid-bound MSP2 to be undetectable, while those regions of MSP2 not involved in the interaction were expected to retain their flexibility, and thus to retain the chemical shift and relaxation properties of free MSP2 [33]. Consistent with these expectations, we saw no changes in chemical shift upon addition of lipid SUVs to MSP2 but a reduction of peak intensity for resonances corresponding to the conserved N-terminal region (Supplementary Figure S2). In the presence of 7.5 mM DLPC as SUVs (protein:lipid molar ratio of 1:60), a uniform reduction in peak intensities of ~20% was observed for residues of the conserved N-terminal region. In the limit of slow exchange, the fractional change in peak intensity reflects the proportion of MSP2 that is bound to the lipid membrane. In this case, however, we cannot rule out a contribution of relaxation due to intermediate exchange to the observed signal attenuation. Nonetheless, it is apparent that under accessible lipid concentrations, the fraction of MSP2 that is lipid bound is relatively low, suggesting that the N-terminus of MSP2 interacts only weakly with this bilayer system. It must be stressed, however, that these observations were made in the absence of the GPI anchor which tethers

Table 1
Structure statistics for final 20 structures.

No. of conformational restraints	
Total no. of distance restraints	591
Intraresidue ($i=j$)	202
Sequential ($\|i–j\|=1$)	196
Medium-range ($1<\|i–j\|<5$)	189
Long-range ($\|i–j\|>4$)	4
No. of dihedral restraints	
Energies[a]	
E_{NOE} (kcal mol^{-1})	6.4 ± 1.7
$E_{dihedral}$ (kcal mol^{-1})	0.20 ± 0.16
RMS deviations from experimental data	
NOEs (Å)	0.019 ± 0.003
Dihedrals (°)	0.27 ± 0.13
Deviations from ideal[b]	
Angles (°)	0.48 ± 0.01
Bonds (Å)	0.003
Impropers (°)	0.35 ± 0.02
Atomic RMS deviations (Å)[c]	
all heavy atoms	1.3 ± 0.5
Backbone heavy atoms, residues 7–24	0.41 ± 0.15
Ramachandran plot[d]	
Most favoured (%)	71.7
Allowed (%)	26.9
Additionally allowed (%)	1.0
Disallowed (%)	0.4

[a] The values for E_{NOE} are calculated from a square well potential with force constants of 30 kcal mol^{-1} $Å^{-2}$.
[b] The values for the bonds, angles, and impropers show the RMS deviations from ideal covalent geometry as defined by the XPLOR forcefield.
[c] The average RMSD to the mean as calculated in MOLMOL.
[d] As reported by PROCHECK-NMR for all residues.

native MSP2 to the merozoite membrane. As discussed below, the presence of the GPI anchor would be expected to substantially enhance the effect of these weak lipid interactions.

3.4. Structure of DPC-bound MSP2 N-terminus

To obtain more information on the structural changes in the N-terminus, we titrated DPC into a solution of a recombinant peptide containing only residues 1–25 of full-length MSP2. As described previously by Low et al. [20], this peptide is conformationally very similar to the corresponding region of full-length recombinant MSP2, as demonstrated, for example, by very similar chemical shifts. On addition of DPC, the backbone amide resonances of $MSP2_{1\text{-}25}$ underwent similar chemical shift changes to those seen for the full-length protein (Fig. 4), even though the titration with full-length MSP2 could not be followed to completion because of excessive line broadening at the higher DPC concentrations. Thus, we conclude that the N-terminus of full-length MSP2 undergoes a conformational transition corresponding to that observed for $MSP2_{1\text{-}25}$, and the shorter construct therefore represents an excellent model of this transition and the underlying lipid interactions. Importantly, the degree of line broadening observed for $MSP2_{1\text{-}25}$ on addition of DPC is significantly less than that observed for full-length MSP2 (Fig. 4 and Supplementary Figure S3), permitting a more detailed structural investigation using this construct. The observed differences in line broadening are consistent with a slower on-rate for full-length MSP2 owing to its slower translational diffusion.

The structure of $MSP2_{1\text{-}25}$ has been solved using solution NMR methods. The resonance assignments were based on previously published data [20], supported by 3D HNCA/HNCO spectra of a $^{13}C/^{15}N$-labelled $MSP2_{1\text{-}25}$ sample. Chemical shift assignments are documented in Supplementary Table I. All NOE-based structural restraints were generated from high-resolution 2D NOESY data. We used a number of different samples to collect information on the system, including unlabelled synthetic material as well as labelled recombinant MSP2. Only very limited changes were observed between the different samples and all NOE restraints were based on one sample only.

Throughout the peptide, $^{1}H^{\alpha}$ and $^{13}C^{\alpha}$ chemical shifts show characteristic deviations from random-coil values, indicative of α-helical structure (Fig. 5A and Supplementary Figure S4). These deviations are particularly pronounced for residues 10–22, and are supported by i to $i+3$ NOE connectivities in this region (Fig. 5). Backbone torsion angle restraints were therefore used to maintain helical conformation in this region. The final structural ensemble was calculated using 591 NOE restraints, and 37 torsion angle restraints. As seen in Fig. 7, the peptide adopts an α-helical structure along essentially its full length, though the helical structure is rather poorly defined in the N-terminal 7 residues (Supplementary Figure S5). The few long-range NOEs observed were between the side chains of residues 12 and 17, consistent with the extended helical structure. We have

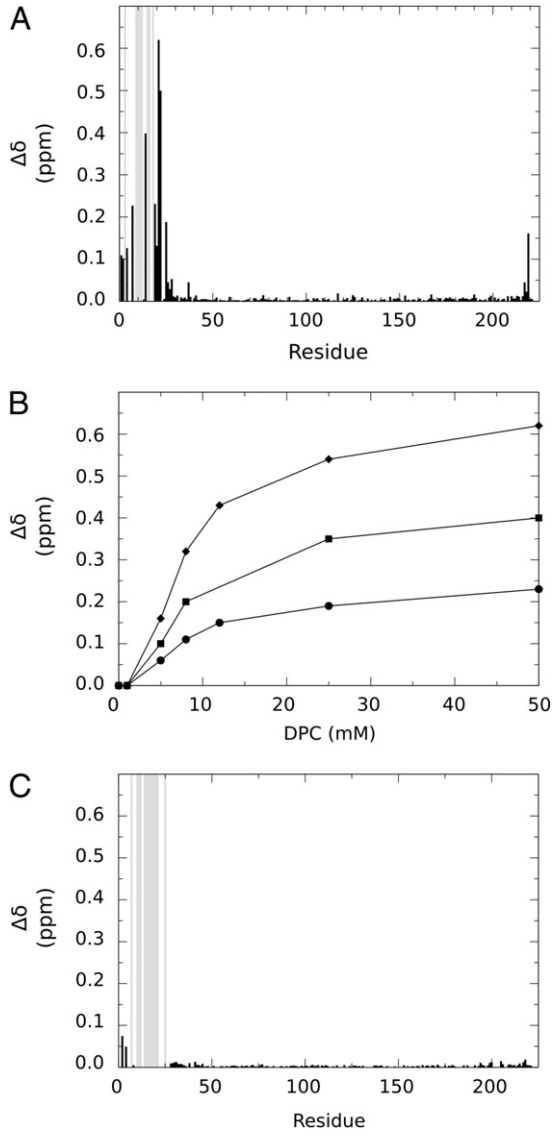

Fig. 2. Backbone amide chemical shift changes ($\Delta\delta=[(\Delta\delta_N/5)^2+(\Delta\delta_{HN})^2]^{1/2}$) for MSP2 on titration with DPC. A: Chemical shift changes in the presence of 50 mM DPC in 10 mM sodium acetate, pH 4.5. for each assigned backbone amide resonance are plotted as black bars. Grey bars denote resonances that are broadened beyond detection under these conditions. B: DPC concentration dependence of chemical shift changes for residues 7 (●), 14(■) and 21 (♦) in 10 mM sodium acetate, pH 4.5. C: Chemical shift changes for MSP2 in the presence of 20 mM DPC in 10 mM sodium phosphate, pH 7.3. Chemical shift changes for each assigned backbone amide resonance are plotted as black bars. Grey bars denote resonances that are broadened beyond detection under these conditions.

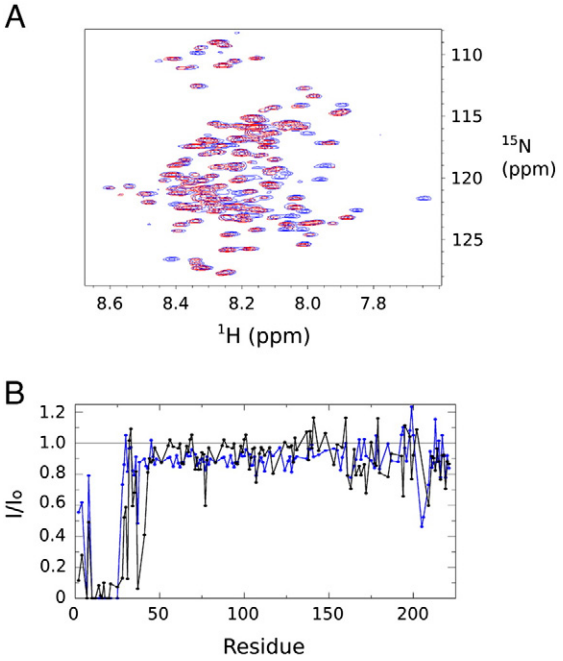

Fig. 3. A. ^{1}H–^{15}N HSQC of 0.2 mM FC27 MSP2 in 10 mM sodium phosphate, pH 7.3, in the presence (red) and absence (blue) of 2.4 mM LPPG. B. Peak intensities for well-resolved backbone amide resonances in the presence of 2.4 mM LPPG (black), and in the presence of 20 mM DPC (blue) in 10 mM sodium phosphate, pH 7.3, normalised relative to lipid-free peak intensities.

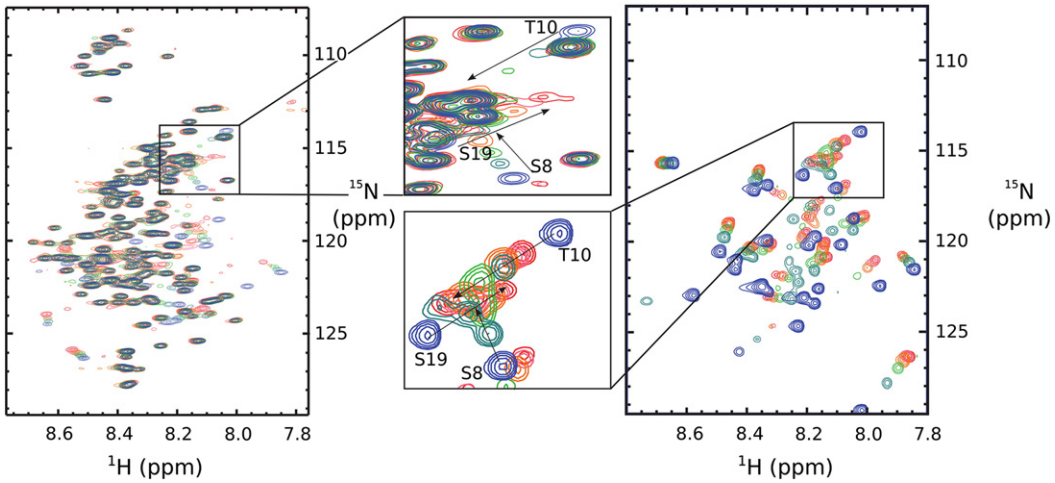

Fig. 4. ^{1}H–^{15}N HSQC titration of full-length FC27 MSP2 (left panel) and MSP2$_{1\text{-}25}$ (right panel) with DPC. Spectra were acquired at 25 °C in 20 mM sodium acetate, pH 4.5, with 0 mM (blue), 5 mM (teal), 8 mM (green), 12 mM (orange), 25 mM (pink) and 50 mM (red) DPC.

recently explored the effect of co-solvents including trifluroethanol (TFE) on the aggregation properties of MSP2 [34]. TFE induces helical structure in the N-terminus of MSP2, and the structure of MSP2$_{1\text{-}25}$ in 50% TFE is similar in many respects to that described here, with a well-defined helical conformation observed in the C-terminal two-thirds of the peptide. As noted in the context of the TFE structure, this helix is imperfectly amphipathic; in the current structure two distinct hydrophobic faces can be detected on the helix, differing in their orientation by ~90° (Fig. 6B).

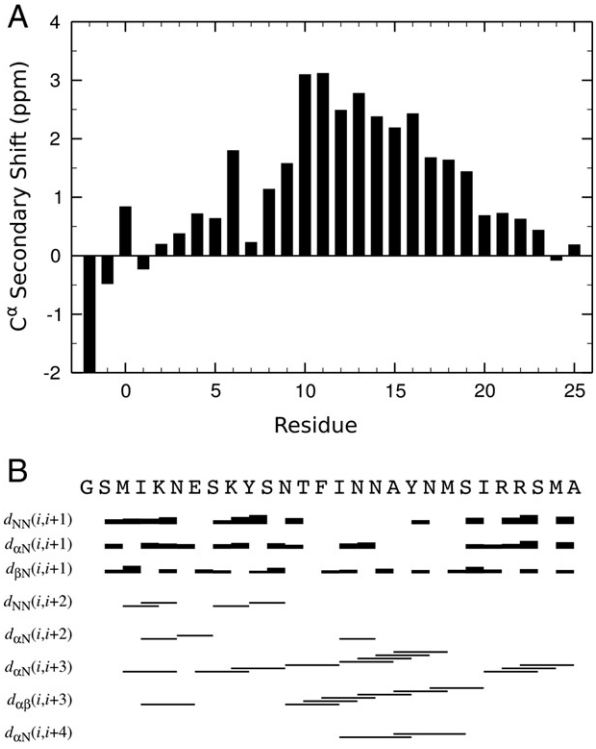

Fig. 5. Secondary C^{α} chemical shifts (A) and summary of sequential and medium range NOEs (B) measured for recombinant MSP2$_{1\text{-}25}$ in the presence of 50 mM DPC, pH 4.5 at 25 °C. Residue numbering is as for full-length MSP2, with the vector-derived N-terminal residues GSM numbered -2, -1 and 0.

4. Discussion

Despite its status as an important candidate for inclusion in a malaria vaccine, little is known of the structural properties of MSP2 on the merozoite surface, or of the implications of these properties for the development of a protective immune response [1]. In particular, it is unclear how MSP2 interacts with the merozoite plasma membrane to which it is GPI anchored. GPI-mediated lipid interactions alter the antigenic properties of proteins of other parasitic organisms [19], but this has not been studied in the case of MSP2 or other malaria antigens. To begin to address these issues, we have probed the interactions of recombinant MSP2 with lipid-mimetic micelles and lipid bilayers using NMR spectroscopy. We observe a consistent interaction of the conserved N-terminal region of MSP2 to these lipids over a range of pH values and diverse lipid head-groups. Although line broadening, most likely the result of intermediate time-scale exchange between free and bound MSP2, has limited our ability to characterise in detail the structure of full-length MSP2-lipid complexes, we have established that an N-terminal fragment of MSP2 serves as an excellent model of these complexes.

Although the interactions we characterise here are of relatively low apparent affinity, the fact that MSP2 is covalently attached to the merozoite membrane by its C-terminal GPI anchor strongly enhances the likelihood that such interactions might modulate the conformational and immunogenic properties of MSP2 on the merozoite surface. Assuming that the ~200 residues of MSP2 between the N-terminal region and the GPI anchor resemble a random coil, as they do for the recombinant protein *in vitro* [18], the MSP2 N-terminus is free to sample a hemispherical region near the site of the C-terminal anchor of RMS radius ~12 nm [35], giving an effective concentration of the N-terminus at the membrane of the order of 1 mM. Under these conditions even weak lipid-MSP2 interactions will be significantly populated. A possible model of MSP2 on the merozoite surface that is consistent with our observations is shown in Fig. 7, although we note that MSP2 may populate other states, including self-associated species [17].

Several lines of evidence suggest that the central variable region dominates the immune response to MSP2 in natural protective immunity against malaria [15], and in those vaccinated with MSP2 [12]. The mechanism by which the conserved N- and C-terminal regions of MSP2 are apparently protected from immune recognition remains obscure. The results presented here allow us to suggest that interactions with the merozoite surface membrane may have a role in mediating

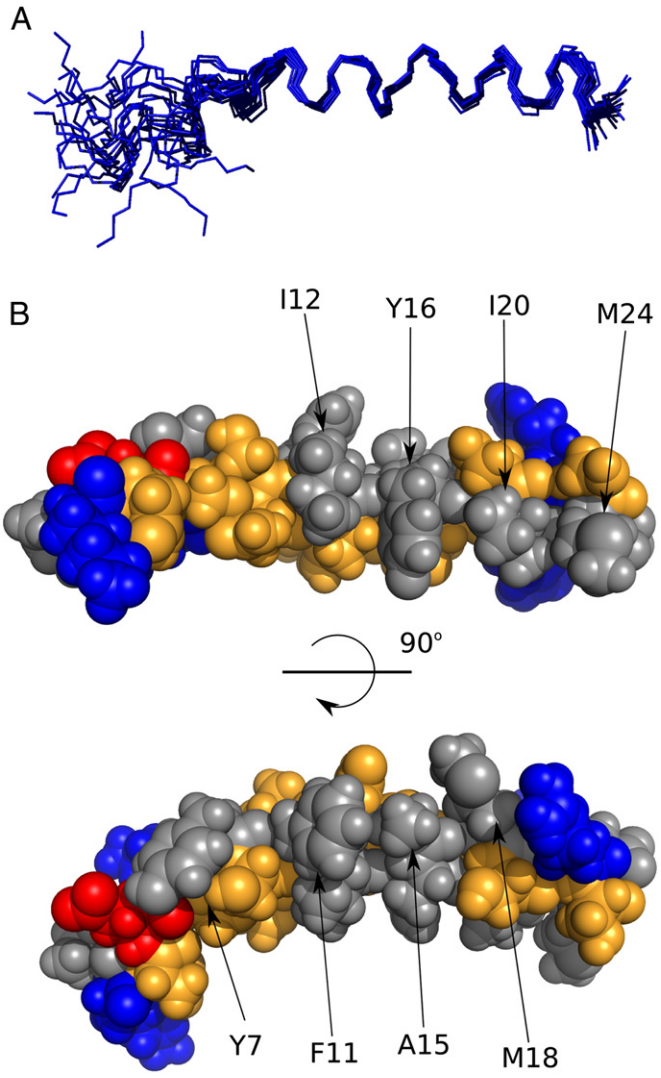

Fig. 6. NMR structure of $MSP2_{1-25}$ in DPC micelles. A. C^{α} trace of the ensemble of 20 calculated structures, superimposed over residues 7–24. B. Space filling model of the closest to average structure in the same orientation as A (top) and rotated by 90° about the helical axis (bottom). Hydrophobic residues are grey, neutral hydrophilic residues gold, acidic residues red and basic residues blue. Residues comprising the two hydrophobic faces are labelled.

this effect, at least in the case of the N-terminal region. Such protection may be mediated by the conformational transition that accompanies lipid binding, as the N-terminal region of lipid-free MSP2 populates the helical state only very weakly. Alternatively, lipid interactions may offer protection from immune surveillance by way of simple occlusion of antibodies from the juxtamembrane region by the dense proteinaceous coat that surrounds the merozoite [36]. This later possibility seems less likely given that antibodies to juxtamembrane domains of other merozoite antigens including MSP1 and AMA1 recognise the merozoite surface and inhibit parasite growth [37,38]. It will be of interest, therefore, to explore the role of lipid interactions and the GPI anchor in modulating the immune response to MSP2, with a view to developing MSP2-based antigens better able to mimic the natural immune response and leading to a more effective malaria vaccine.

Acknowledgements

We thank Shenggen Yao for helpful discussions about diffusion measurements. This work was supported in part by grants to R.F.A. and R.S.N. from the National Health and Medical Research Council of Australia (Project grant 637368), and to M.Ø.P from the Danish Council for Independent Research|Natural Sciences (project grant 09-070284). R.S.N. acknowledges fellowship support from the NHMRC.

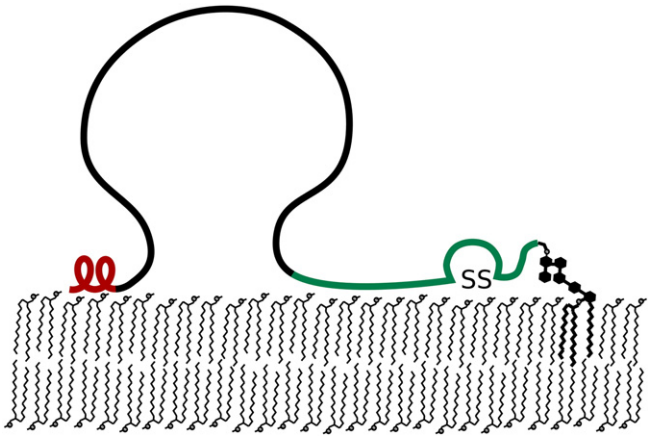

Fig. 7. A possible model of MSP2 on the merozoite surface. The conserved N-terminal region (red) is stabilized as a helix by lipid interactions, and the C-terminal region (green) is proximal to the membrane due to the GPI anchor. The central variable region is exposed to the host immune system.

Appendix A. Supplementary data

Supplementary data to this article can be found online at http://dx.doi.org/10.1016/j.bbamem.2012.06.015.

References

[1] R.F. Anders, C.G. Adda, M. Foley, R.S. Norton, Recombinant protein vaccines against the asexual blood-stages of *Plasmodium falciparum*, Hum. Vaccin. 6 (2010) 39–53.
[2] J.A. Smythe, R.L. Coppel, G.V. Brown, R. Ramasamy, D.J. Kemp, R.F. Anders, Identification of two integral membrane proteins of *Plasmodium falciparum*, Proc. Natl. Acad. Sci. U.S.A. 85 (1988) 5195–5199.
[3] P.R. Gilson, T. Nebl, D. Vukcevic, R.L. Moritz, T. Sargeant, T.P. Speed, L. Schofield, B.S. Crabb, Identification and stoichiometry of glycosylphosphatidylinositol-anchored membrane proteins of the human malaria parasite *Plasmodium falciparum*, Mol. Cell Proteomics 5 (2006) 1286–1299.
[4] F. Al-Yaman, B. Genton, R.F. Anders, M. Falk, T. Triglia, D. Lewis, J. Hii, H.P. Beck, M.P. Alpers, Relationship between humoral response to *Plasmodium falciparum* merozoite surface antigen-2 and malaria morbidity in a highly endemic area of Papua New Guinea, Am. J. Trop. Med. Hyg. 51 (1994) 593–602.
[5] F. Al-Yaman, B. Genton, R. Anders, J. Taraika, M. Ginny, S. Mellor, M.P. Alpers, Assessment of the role of the humoral response to *Plasmodium falciparum* MSP2 compared to RESA and SPf66 in protecting Papua New Guinean children from clinical malaria, Parasite Immunol. 17 (1995) 493–501.
[6] R.R. Taylor, S.J. Allen, B.M. Greenwood, E.M. Riley, IgG3 antibodies to *Plasmodium falciparum* merozoite surface protein 2 (MSP2): increasing prevalence with age and association with clinical immunity to malaria, Am. J. Trop. Med. Hyg. 58 (1998) 406–413.
[7] W.G. Metzger, D.M. Okenu, D.R. Cavanagh, J.V. Robinson, K.A. Bojang, H.A. Weiss, J.S. McBride, B.M. Greenwood, D.J. Conway, Serum IgG3 to the *Plasmodium falciparum* merozoite surface protein 2 is strongly associated with a reduced prospective risk of malaria, Parasite Immunol. 25 (2003) 307–312.
[8] S.D. Polley, D.J. Conway, D.R. Cavanagh, J.S. McBride, B.S. Lowe, T.N. Williams, T.W. Mwangi, K. Marsh, High levels of serum antibodies to merozoite surface protein 2 of *Plasmodium falciparum* are associated with reduced risk of clinical malaria in coastal Kenya, Vaccine 24 (2006) 4233–4246.
[9] D.I. Stanisic, J.S. Richards, F.J. McCallum, P. Michon, C.L. King, S. Schoepflin, P.R. Gilson, V.J. Murphy, R.F. Anders, I. Mueller, J.G. Beeson, Immunoglobulin G subclass-specific responses against *Plasmodium falciparum* merozoite antigens are associated with control of parasitemia and protection from symptomatic illness, Infect. Immunol. 77 (2009) 1165–1174.
[10] B. Genton, F. Al-Yaman, I. Betuela, R.F. Anders, A. Saul, K. Baea, M. Mellombo, J. Taraika, G.V. Brown, D. Pye, D.O. Irving, I. Felger, H.P. Beck, T.A. Smith, M.P. Alpers, Safety and immunogenicity of a three-component blood-stage malaria vaccine (MSP1, MSP2, RESA) against *Plasmodium falciparum* in Papua New Guinean children, Vaccine 22 (2003) 30–41.
[11] J.S. McCarthy, J. Marjason, S. Elliott, P. Fahey, G. Bang, E. Malkin, E. Tierney, H. Aked-Hurditch, C. Adda, N. Cross, J.S. Richards, F.J. Fowkes, M.J. Boyle, C. Long, P. Druilhe, J.G. Beeson, R.F. Anders, A phase 1 trial of MSP2-C1, a blood-stage malaria

vaccine containing 2 isoforms of MSP2 formulated with Montanide(R) ISA 720, PLoS One 6 (2011) e24413.
[12] B. Genton, I. Betuela, I. Felger, F. Al-Yaman, R.F. Anders, A. Saul, L. Rare, M. Baisor, K. Lorry, G.V. Brown, D. Pye, D.O. Irving, T.A. Smith, H.P. Beck, M.P. Alpers, A recombinant blood-stage malaria vaccine reduces *Plasmodium falciparum* density and exerts selective pressure on parasite populations in a phase 1-2b trial in Papua New Guinea, J. Infect. Dis. 185 (2002) 820–827.
[13] B. Fenton, J.T. Clark, C.F. Wilson, J.S. McBride, D. Walliker, Polymorphism of a 35-48 kDa *Plasmodium falciparum* merozoite surface antigen, Mol. Biochem. Parasitol. 34 (1989) 79–86.
[14] J.A. Smythe, R.L. Coppel, K.P. Day, R.K. Martin, A.M. Oduola, D.J. Kemp, R.F. Anders, Structural diversity in the *Plasmodium falciparum* merozoite surface antigen 2, Proc. Natl. Acad. Sci. U.S.A. 88 (1991) 1751–1755.
[15] N. Lawrence, A. Stowers, V. Mann, D. Taylor, A. Saul, Recombinant chimeric proteins generated from conserved regions of *Plasmodium falciparum* merozoite surface protein 2 generate antiparasite humoral responses in mice, Parasite Immunol. 22 (2000) 211–221.
[16] C.G. Adda, C.A. MacRaild, L. Reiling, K. Wycherley, M.J. Boyle, M. Foley, J.G. Beeson, R.S. Norton, R.F. Anders, Antigenic characterisation of an intrinsically unstructured protein: *Plasmodium falciparum* merozoite surface protein 2, (submitted for publication).
[17] C.G. Adda, V.J. Murphy, M. Sunde, L.J. Waddington, J. Schloegel, G.H. Talbo, K. Vingas, V. Kienzle, R. Masciantonio, G.J. Howlett, A.N. Hodder, M. Foley, R.F. Anders, *Plasmodium falciparum* merozoite surface protein 2 is unstructured and forms amyloid-like fibrils, Mol. Biochem. Parasitol. 166 (2009) 159–171.
[18] X. Zhang, M.A. Perugini, S. Yao, C.G. Adda, V.J. Murphy, A. Low, R.F. Anders, R.S. Norton, Solution conformation, backbone dynamics and lipid interactions of the intrinsically unstructured malaria surface protein MSP2, J. Mol. Biol. 379 (2008) 105–121.
[19] P. Butikofer, T. Malherbe, M. Boschung, I. Roditi, GPI-anchored proteins: now you see'em, now you don't, FASEB J. 15 (2001) 545–548.
[20] A. Low, I.R. Chandrashekaran, C.G. Adda, S. Yao, J.K. Sabo, X. Zhang, A. Soetopo, R.F. Anders, R.S. Norton, Merozoite surface protein 2 of *Plasmodium falciparum*: expression, structure, dynamics, and fibril formation of the conserved N-terminal domain, Biopolymers 87 (2007) 12–22.
[21] D.S. Wishart, C.G. Bigam, J. Yao, F. Abildgaard, H.J. Dyson, E. Oldfield, J.L. Markley, B.D. Sykes, ^{1}H, ^{13}C and ^{15}N chemical shift referencing in biomolecular NMR, J. Biomol. NMR 6 (1995) 135–140.
[22] S. Yao, G.J. Howlett, R.S. Norton, Peptide self-association in aqueous trifluoroethanol monitored by pulsed field gradient NMR diffusion measurements, J. Biomol. NMR 16 (2000) 109–119.
[23] F. Delaglio, S. Grzesiek, G.W. Vuister, G. Zhu, J. Pfeifer, A. Bax, NMRPipe: a multidimensional spectral processing system based on UNIX pipes, J. Biomol. NMR 6 (1995) 277–293.
[24] T.D. Goddard, D.G. Kneller, SPARKY 3, University of California, San Francisco, 2006.
[25] S. Ludvigsen, F.M. Poulsen, Positive theta-angles in proteins by nuclear magnetic resonance spectroscopy, J. Biomol. NMR 2 (1992) 227–233.
[26] C.D. Schwieters, J.J. Kuszewski, N. Tjandra, G.M. Clore, The Xplor-NIH NMR molecular structure determination package, J. Magn. Reson. 160 (2003) 65–73.
[27] R.A. Laskowski, J.A. Rullmannn, M.W. MacArthur, R. Kaptein, J.M. Thornton, AQUA and PROCHECK-NMR: programs for checking the quality of protein structures solved by NMR, J. Biomol. NMR 8 (1996) 477–486.
[28] R. Koradi, M. Billeter, K. Wüthrich, MOLMOL: a program for display and analysis of macromolecular structures, J. Mol. Graph. 14 (1996) 51–55.
[29] W.L. DeLano, The PyMOL Molecular Graphics System, DeLano Scientific, Palo Alto, CA, 2002.
[30] R.D. Krueger-Koplin, P.L. Sorgen, S.T. Krueger-Koplin, An evaluation of detergents for NMR structural studies of membrane proteins, J. Biomol. NMR (2004) 43–57.
[31] Q. Zhang, H.S. Atreya, D.E. Kamen, M.E. Girvin, T. Szyperski, GFT projection NMR based resonance assignment of membrane proteins: application to subunit C of E. coli F(1)F (0) ATP synthase in LPPG micelles, J. Biomol. NMR 40 (2008) 157–163.
[32] J.J. Chou, J.L. Baber, A. Bax, Characterization of phospholipid mixed micelles by translational diffusion, J. Biomol. NMR 29 (2004) 299–308.
[33] C.R. Bodner, C.M. Dobson, A. Bax, Multiple tight phospholipid-binding modes of α-synuclein revealed by solution NMR spectroscopy, J. Mol. Biol. 390 (2009) 775–790.
[34] X. Zhang, C.G. Adda, A. Low, J. Zhang, W. Zhang, H. Sun, X. Tu, R.F. Anders, R.S. Norton, Role of helical structure of the N-terminal region of *Plasmodium falciparum* merozoite surface protein 2 (MSP2) in fibril formation and membrane interaction, Biochemistry 51 (2012) 1380–1387.
[35] C. Tanford, K. Kawahara, S. Lapanje, Proteins in 6-M guanidine hydrochloride. Demonstration of random coil behavior, J. Biol. Chem. 241 (1966) 1921–1923.
[36] L.H. Bannister, G.H. Mitchell, G.A. Butcher, E.D. Dennis, S. Cohen, Structure and development of the surface coat of erythrocytic merozoites of *Plasmodium knowlesi*, Cell Tissue Res. 245 (1986) 281–290.
[37] M.J. Blackman, H.G. Heidrich, S. Donachie, J.S. McBride, A.A. Holder, A single fragment of a malaria merozoite surface protein remains on the parasite during red cell invasion and is the target of invasion-inhibiting antibodies, J. Exp. Med. 172 (1990) 379–382.
[38] M. Nair, M.G. Hinds, A.M. Coley, A.N. Hodder, M. Foley, R.F. Anders, R.S. Norton, Structure of domain III of the blood-stage malaria vaccine candidate, *Plasmodium falciparum* apical membrane antigen 1 (AMA1), J. Mol. Biol. 322 (2002) 741–753.